doi:10.1093/brain/aww008 BRAIN 2016: 139; 1164–1179 | 1164

BRAIN
A JOURNAL OF NEUROLOGY

# White matter hyperintensities and imaging patterns of brain ageing in the general population

**Mohamad Habes,[1,2,3] Guray Erus,[2] Jon B. Toledo,[4] Tianhao Zhang,[2] Nick Bryan,[2] Lenore J. Launer,[5] Yves Rosseel,[6] Deborah Janowitz,[3] Jimit Doshi,[2] Sandra Van der Auwera,[3,7] Bettina von Sarnowski,[8] Katrin Hegenscheid,[9] Norbert Hosten,[9] Georg Homuth,[10] Henry Völzke,[1] Ulf Schminke,[8] Wolfgang Hoffmann,[1,7] Hans J. Grabe[3,7,*] and Christos Davatzikos[2,*]**

[*]These authors contributed equally to this work.

White matter hyperintensities are associated with increased risk of dementia and cognitive decline. The current study investigates the relationship between white matter hyperintensities burden and patterns of brain atrophy associated with brain ageing and Alzheimer's disease in a large populatison-based sample ($n = 2367$) encompassing a wide age range (20–90 years), from the Study of Health in Pomerania. We quantified white matter hyperintensities using automated segmentation and summarized atrophy patterns using machine learning methods resulting in two indices: the SPARE-BA index (capturing age-related brain atrophy), and the SPARE-AD index (previously developed to capture patterns of atrophy found in patients with Alzheimer's disease). A characteristic pattern of age-related accumulation of white matter hyperintensities in both periventricular and deep white matter areas was found. Individuals with high white matter hyperintensities burden showed significantly ($P < 0.0001$) lower SPARE-BA and higher SPARE-AD values compared to those with low white matter hyperintensities burden, indicating that the former had more patterns of atrophy in brain regions typically affected by ageing and Alzheimer's disease dementia. To investigate a possibly causal role of white matter hyperintensities, structural equation modelling was used to quantify the effect of Framingham cardiovascular disease risk score and white matter hyperintensities burden on SPARE-BA, revealing a statistically significant ($P < 0.0001$) causal relationship between them. Structural equation modelling showed that the age effect on SPARE-BA was mediated by white matter hyperintensities and cardiovascular risk score each explaining 10.4% and 21.6% of the variance, respectively. The direct age effect explained 70.2% of the SPARE-BA variance. Only white matter hyperintensities significantly mediated the age effect on SPARE-AD explaining 32.8% of the variance. The direct age effect explained 66.0% of the SPARE-AD variance. Multivariable regression showed significant relationship between white matter hyperintensities volume and hypertension ($P = 0.001$), diabetes mellitus ($P = 0.023$), smoking ($P = 0.002$) and education level ($P = 0.003$). The only significant association with cognitive tests was with the immediate recall of the California verbal and learning memory test. No significant association was present with the APOE genotype. These results support the hypothesis that white matter hyperintensities contribute to patterns of brain atrophy found in beyond-normal brain ageing in the general population. White matter hyperintensities also contribute to brain atrophy patterns in regions related to Alzheimer's disease dementia, in agreement with their known additive role to the likelihood of dementia. Preventive strategies reducing the odds to develop cardiovascular disease and white matter hyperintensities could decrease the incidence or delay the onset of dementia.

1 Institute for Community Medicine, University of Greifswald, Germany
2 Centre for Biomedical Image Computing and Analytics, University of Pennsylvania, USA
3 Department of Psychiatry, University of Greifswald, Germany

Received May 29, 2015. Revised November 13, 2015. Accepted December 17, 2015. Advance Access publication February 24, 2016

4 Department of Pathology and Laboratory Medicine, Institute on Aging, Center for Neurodegenerative Disease Research, University of Pennsylvania, USA
5 Laboratory of Epidemiology, Demography, and Biometry, National Institute on Aging, USA
6 Department of Data Analysis, Ghent University, Belgium
7 German Centre for Neurodegenerative Diseases (DZNE), Rostock/Greifswald, Germany
8 Department of Neurology, University of Greifswald, Germany
9 Department of Radiology, University of Greifswald, Germany
10 Institute for Genetics and Functional Genomics, University of Greifswald, Germany

Correspondence to: Mohamad Habes,
3700 Hamilton Walk, Department of Radiology,
University of Pennsylvania,
19104 Philadelphia,
USA
E-mail: habesm@uphs.upenn.edu

**Keywords:** white matter hyperintensities; Alzheimer's disease; brain ageing; cardiovascular disease; mild cognitive impairment

**Abbreviations:** CVD-RS = cardiovascular disease risk score; ODVBA = optimal-discriminative voxel-based analysis; SPARE-AD = spatial pattern of abnormality for recognition of early Alzheimer's disease; SPARE-BA = spatial pattern of atrophy for recognition of brain ageing; SHIP = Study of Health in Pomerania; WMH = white matter hyperintensities

# Introduction

White matter hyperintensities (WMH), which are typically detected on fluid-attenuated inversion recovery (FLAIR) brain MRI, are common findings in older adults. WMH are considered a type of sporadic small vessel disease (Wardlaw and Pantoni, 2014). The aetiology and the pathophysiology of WMH are not yet completely understood. Pathological substrates of WMH are heterogeneous in nature and severity (Gouw *et al.*, 2011). Previous studies proposed that axonal loss and demyelination contribute to the appearance of WMH, which could be a consequence of chronic ischaemia caused by cerebral small vessel disease (Prins and Scheltens, 2015). Others suggest hypoperfusion due to altered cerebrovascular autoregulation or dysfunction of blood–brain barrier (Simpson *et al.*, 2007), inflammation and amyloid angiopathy (Gouw *et al.*, 2011).

In addition to the poorly understood pathophysiological aetiology of WMH, their relationship with vascular risk factors is not completely uncovered. Sporadic small vessel disease is often proposed to be associated with hypertension (Dufouil *et al.*, 2001); however, it occurs in normotensive patients as well (Wardlaw *et al.*, 2013). Major vascular risk factors such as smoking and diabetes mellitus are also associated with increased WMH volume (Jeerakathil *et al.*, 2004; Jongen *et al.*, 2007). Finally age, which is a key vascular risk factor, is also a consistent risk for WMH (Grueter and Schulz, 2012; Prins and Scheltens, 2015).

Structural brain changes related to ageing (referred to as 'brain ageing' herein) are associated with pronounced grey matter loss, particularly in frontal and parietal lobes (Rachael *et al.*, 2003; Resnick *et al.*, 2003). Recent studies showed distributed patterns of age-related predominant subcortical atrophy, as well as more localized patterns in regions such as amygdala, striatum, prefrontal, cerebellum and in the midline structures, cingulate cortex and precuneus (Draganski *et al.*, 2011). Age-related changes in the brain vary in trajectories across the different regions (Raz *et al.*, 2010). Brain ageing may be associated with a number of possible underlying neuropathologic mechanisms such as synapse loss, vascular pathology (Debette *et al.*, 2011) and small vessel disease (Jagust, 2013). Previous studies showed that high WMH burden was correlated with total grey matter atrophy (Aribisala *et al.*, 2013; Wang *et al.*, 2014) and atrophy in regions like the temporal lobe (Tuladhar *et al.*, 2015; Wen *et al.*, 2006), and the frontal cortex (Raji *et al.*, 2012). The spatial patterns of brain atrophy associated with higher volume of WMH and advanced brain ageing (deviated from normative age-related atrophy patterns) are still not well understood in the general population.

Additional studies have shown links between WMH and the presence of Alzheimer's disease pathology (Brickman *et al.*, 2015; Prins and Scheltens, 2015) and cognitive decline (Carmichael *et al.*, 2010; Vermeer *et al.*, 2003; van der Flier *et al.*, 2005). WMH were associated with grey matter atrophy in Alzheimer's disease-related regions such as medial temporal (Appel *et al.*, 2009), and it was proposed that the appearance of WMH doubles the risk of dementia (Wardlaw *et al.*, 2015). The overlap between WMH- and dementia-related atrophy patterns should be better understood, as the additional atrophy induced by WMH in regions typically affected by dementia, is likely to impose an additive effect on symptoms caused by the dementia pathology itself.

We hypothesized that WMH are partially associated with brain atrophy patterns seen in older individuals and in Alzheimer's disease dementia. The goals of our analysis were to evaluate the association of WMH with advanced brain ageing and elucidate the WMH proportion in mediating the age effect on the atrophy related to brain ageing

in a large ageing sample from the adult general population. Towards this hypothesis we summarized patterns of brain atrophy using two indices (Fan *et al.*, 2007; Klöppel *et al.*, 2008; Franke *et al.*, 2010; Gaser *et al.*, 2013): the SPARE-BA index (capturing age-related brain atrophy), and the SPARE-AD index (previously developed to capture patterns of atrophy found in patients with Alzheimer's disease) (Davatzikos *et al.*, 2009), and examined whether individuals with high WMH burden displayed differences in those defined patterns.

# Materials and methods

## Participants of SHIP

We included in this study 2367 subjects from the SHIP (Study of Health in Pomerania) cohort, led by the Institute for Community Medicine at the Medical Faculty of the University of Greifswald. SHIP started at baseline with SHIP-0 between 1997 and 2001. From 2008 to 2013 the second follow-up examination SHIP-2 was carried out. Concurrent with SHIP-2 a new sample from the same area was drawn and similar examinations were undertaken between 2008 and 2012 (SHIP-Trend). SHIP-2 and SHIP-Trend included whole-body MRI scans (Hegenscheid *et al.*, 2009; Völzke *et al.*, 2011; Habes *et al.*, 2013). Supplementary Fig. 1 shows a flowchart for the included subjects. Table 1 presents a complete description for the sample included in this study. Supplementary Table 1 shows the characteristics of all excluded cases and compares them to the final sample included in the study. The Ethics Committee of the Medical Faculty of the University of Greifswald approved the SHIP study.

## Data assessment in SHIP

Clinical data were collected by a computer-assisted face-to-face interview. We divided smoking in three categories, specifically: current smoking, former smoking, and never smoked. We subdivided the highest attained level of school education into three categories: $<8$ years, 8–10 years, and $>10$ years. For the assessment of leisure time physical activity (sportive exercise, e.g. jogging) we specified the following groups: no activity, low ($>0$–1 h/week), moderate (1–2 h/week) and high ($>2$ h/week) activity in summer and in winter.

Having completed the interview, participants underwent medical examinations: including the measurement of height and weight (continuous variable). Waist circumference was measured in cm (continuous variable). After a 5-min resting period, blood pressure was measured three times on the right arm of seated subjects using a digital blood pressure monitor (HEM-705CP, Omron), with each reading being followed by a further resting period of 3 min. Cuffs were applied according to the circumference of the participant's arm. The mean of the second and third measurements (mmHg) was used for the analyses (continuous variables). All subjects were informed to bring in the packaging of all medication taken during the last 7 days, as well as their drug prescription sheets. Every compound was recorded. We focused on antihypertensive, anti-diabetic and lipid-lowering drugs, as indicators for cardiovascular disease risk factors in the general population.

In SHIP two cognitive tests were obtained: the verbal learning and memory test (the German version for California verbal learning and memory test) (Woods *et al.*, 2006) for the sub-cohort SHIP-2 ($n = 730$), and the Nurnberg age inventory for the sub-cohort SHIP-Trend ($n = 1637$. The Nurnberg age inventory is a German test developed to measure the cognition abilities during brain ageing (Fleischmann and Oswald, 1999). The verbal learning and memory test and Nurnberg age inventory consist of subtests, including immediate and delayed memory tests. Carotid artery stenosis was assessed in SHIP (Supplementary material) and available for 2360 participants, *APOE* genotype was available for 1472 individuals. A complete description of genotyping in SHIP can be found in the Supplementary material.

## Laboratory work

Glycated haemoglobin (HbA1c, measured in %) concentrations were determined with high-performance liquid chromatography (Bio-Rad Diamat). High-density lipoprotein cholesterol concentrations were measured photometrically (Hitachi 704, Roche). HbA1c, total cholesterol, low-density lipoprotein and high-density lipoprotein were measured as dimensional scores.

## Image acquisition

We used $T_1$-weighted and FLAIR MRI to measure regional patterns of WMH as well as ageing-related brain atrophy. The image acquisition parameters have been described in Hegenscheid *et al.* (2009) for SHIP. Briefly, all images were obtained using a 1.5 T Siemens MRI scanner (Magnetom Avanto, Siemens Medical Systems) with an axial MPRAGE sequence and the following parameters: $1 \times 1$ mm in-plane spatial resolution, slice thickness = 1.0 mm (flip angle 15°), echo time = 3.4 ms and repetition time = 1900 ms as well as axial $T_2$-FLAIR sequence with the following parameters: $0.9 \times 0.9$ mm in-plane spatial resolution, slice thickness = 3.0 mm (flip angle 15°), echo time = 3250 ms and repetition time = 50 000 ms.

## Image preprocessing

Preprocessing contained the following steps, which were applied on all scans. Multi atlas-based algorithm removed extra-cranial material (skull-stripping) (Doshi *et al.*, 2013). All skull-stripped images were visually inspected for quality control by M.H. and all scans rated as low skull-stripping quality (i.e. over or under-segmented brains) were excluded ($n = 121$). Images were corrected for bias field (Tustison *et al.*, 2010) and tissue segmentation into grey matter, white matter and CSF was performed using an in-house developed algorithm (Li *et al.*, 2014). Finally, intracranial volume was calculated and defined as the total of white matter, grey matter and cortical and ventricular CSF, and has been calculated using the binary brain mask of a subject.

**Table 1 Description of the SHIP sample included in this study**

| Characteristic<br>SHIP subcohort | SHIP-2<br>(*n* = 730) | SHIP-Trend<br>(*n* = 1637) | SHIP study sample<br>(*n* = 2367) |
|---|---|---|---|
| **Age, mean (SD), years** | 55.60 (12.30) | 51.00 (14.06) | 52.42 (13.71) |
| **Gender *n* (%), female** | 399 (54.60) | 920 (56.20) | 1319 (56.72) |
| **Systolic blood pressure, mean (SD), mmHg** | 131.20 (17.98) | 125.54 (17.11) | 127.29 (17.58) |
| **Glycated haemoglobin (HbA1c), mean (SD)** | 5.37 (0.822) | 5.25 (0.70) | 5.29 (0.74) |
| **Total cholesterol, mean (SD), mmol/l** | 5.51 (1.07) | 5.53 (1.07) | 5.52 (1.07) |
| **High-density lipoprotein, mean (SD), mmol/l** | 1.46 (0.38) | 1.46 (0.37) | 1.46 (0.37) |
| **Low-density lipoprotein, mean (SD), mmol/l** | 3.35 (0.93) | 3.42 (0.92) | 3.40 (0.92) |
| **Waist circumference, mean (SD), cm** | 89.77 (12.75) | 88.70 (12.80) | 89.03 (12.79) |
| **Body height, cm** | 169.16 (9.26) | 169.75 (9.22) | 169.57 (9.23) |
| **Education, *n* (%)** | | | |
| <8 years | 135 (18.49) | 234 (14.29) | 369 (15.58) |
| 8–10 years | 420 (57.53) | 900 (54.97) | 1320 (55.76) |
| >10 years | 175 (25.97) | 503 (30.72) | 678 (28.64) |
| **Cigarette smoking, *n* (%)** | | | |
| Never-smoker | 291 (39.86) | 676 (41.29) | 967 (40.85) |
| Ex-smoker | 300 (41.09) | 577 (35.24) | 877 (37.05) |
| Current smoker | 139 (19.04) | 384 (23.45) | 523 (22.09) |
| **Physical activity, *n* (%)** | | | |
| No | 206 (28.21) | 536 (32.74) | 742 (31.34) |
| >0–1 h/week | 111 (15.20) | 256 (15.63) | 367 (15.50) |
| 1–2 h/week | 215 (29.45) | 447 (27.30) | 662 (27.96) |
| >2 h/week | 198 (27.12) | 398 (24.31) | 596 (25.17) |
| **Medication** | | | |
| Anti-diabetics, *n* (%) | 38 (5.20) | 62 (3.78) | 100 (4.22) |
| Antihypertensive, *n* (%) | 269 (36.84) | 504 (30.78) | 773 (32.65) |
| Lipid lowering drugs, *n* (%) | 116 (15.89) | 137 (8.36) | 253 (10.68) |
| **Internal carotid artery stenosis (left or right)**[d] | | | |
| <50%, *n* (%) | 1 (0.13)[a] | 5 (0.30)[b] | 6 (0.25)[c] |
| 50–60%, *n* (%) | 0 (0)[a] | 4 (0.24)[b] | 4 (0.16)[c] |
| 60–70%, *n* (%) | 0 (0)[a] | 3 (0.18)[b] | 3 (0.12)[c] |
| 70–80%, *n* (%)[e] | 0 (0)[a] | 1 (0.06)[b] | 1 (0.04)[c] |
| Occlusion, *n* (%)[e] | 1 (0.13)[a] | 3 (0.18)[b] | 4 (0.16)[c] |
| **Verbal Learning and Memory Test, mean (SD)** | 8.58 (2.97) | | |
| **Nurnberg Age Inventory, mean (SD)** | | 11.23 (2.54) | |

[a,b,c]Measures available for 727, 1633, and 2360, participants, respectively.
[d]According to the European Carotid Surgery Trial criteria.
[e]Considered as clinically relevant and 99.78% from the population are healthy.

## Fully automated WMH segmentation

FLAIR and $T_1$ images were co-registered to the same space. We segmented WMH using a support vector machine-based method (Lao *et al.*, 2008), used in previous studies of a similar nature (Coker *et al.*, 2009; Launer *et al.*, 2011). Minimum WMH volume was set to 25 $mm^3$, to ensure ischaemic origin of the detected hyperintense area. All automatically segmented images were visually inspected for quality control by M.H. and all results rated as low segmentation quality (i.e. over or under-segmented WMH) were excluded ($n = 154$). To visualize the spatial extend of WMH accumulation, we non-linearly aligned individual lesion segmentations to a common template space using the registration method described in Ou *et al.* (2011), and computed lesion frequency maps.

## Calculation of tissue density maps

Images were non-linearly aligned to a standardized brain atlas (Ou *et al.*, 2011), and regional volumetric maps, named RAVENS maps, were calculated (Davatzikos *et al.*, 2001) for grey matter, white matter, CSF and WMH, considering segmented WMH as a distinct tissue class in the generation of RAVENS maps. The RAVENS maps enable direct comparison of tissue distribution on magnetic resonance images of different subjects. The RAVENS approach has been extensively validated and applied to a variety of studies (Davatzikos *et al.*, 2001, 2009; Good *et al.*, 2002; Stewart *et al.*, 2006; Fan *et al.*, 2008). Grey matter RAVENS maps were normalized by intracranial volume to adjust for global differences in head size. Extended information on WMH segmentation and the

generation of RAVENS maps can be found in the Supplementary material.

## MRI pattern classification

Visualizations of statistical parametric maps reflecting spatial patterns of brain atrophy are frequently used in neuroimaging. However, quantifying such patterns and integrating them into indices that can be further related to other relevant measures, such as WMH and clinical measures, is less common. We evaluated the beyond normal brain ageing atrophy patterns in SHIP subjects using a high-dimensional pattern classification methodology, which was initially proposed for quantifying spatial pattern of abnormality for recognition of early Alzheimer's disease (SPARE-AD) (Fan *et al.*, 2007; Davatzikos *et al.*, 2009). The SPARE-AD index is derived from a support vector machines classifier (Vapnik, 1999) trained for optimal discrimination between healthy controls and age-matched Alzheimer's disease patients (Da *et al.*, 2014), summarizes the high dimensional image data with a single score that indicates the distance of the test sample from the classification hyperplane. More positive SPARE-AD implies more Alzheimer's disease-like brain structure, and more negative SPARE-AD implies more normal structure. SPARE-AD scores have been shown to detect earliest preclinical cognitive changes (Toledo *et al.*, 2015) and predict conversion from normal cognition to mild cognitive impairment (Davatzikos *et al.*, 2009; Toledo *et al.*, 2014) and from mild cognitive impairment to Alzheimer's disease dementia (Da *et al.*, 2014; Toledo *et al.*, 2014). We calculated SPARE-AD scores for all SHIP subjects using a linear support vector machines-based model trained on the external training dataset described in Da *et al.* (2014). SPARE-AD corresponds to the volume in the Alzheimer's disease-related regions weighted together demonstrating an Alzheimer's disease signature similar to methods frequently used in the literature (Vemuri *et al.*, 2008; Dickerson *et al.*, 2009; Frisoni *et al.*, 2010; Wirth *et al.*, 2013; Jack *et al.*, 2015). Extended information on the SPARE-AD methodology can be found in the Supplementary material.

We used a similar machine learning methodology for quantifying brain ageing-related atrophy patterns in SHIP subjects, denoted here as SPARE-BA scores. For training the model, a training dataset was constructed by selecting young and old subject groups from the SHIP data, defined as subjects $\leqslant 45$ years ($n = 841$, mean age $\pm$ SD 36.6 $\pm$ 6.2) and subjects $\geqslant 60$ years ($n = 871$, 68.1 $\pm$ 5.6), respectively. Training groups were well balanced in terms of gender (53.6% and 54.3% female in young and old groups, respectively). For all subjects in the training dataset, the SPARE-BA score was calculated with the leave-one-out cross-validation principle to ensure that the SPARE-BA index of each subject was derived from a model that was trained on an independent dataset. For all other subjects (ages 46 to 59), a model trained using the whole training set was used for calculation of the score, since these subjects were by construction different from the training set. Higher (positive) values of SPARE-BA index implied that the subject had less pronounced brain ageing patterns and vice versa for lower (negative) values.

## Cardiovascular disease risk score

To summarize the cardiovascular disease risk profile for every individual in a single score, we calculated the equation of the Framingham risk score (D'Agostino *et al.*, 2008), considering the following risk factors: age, gender, total cholesterol level, high-density lipoprotein, systolic blood pressure, systolic blood pressure treatment status, diabetes mellitus and smoking.

## Statistical analysis

We used ordinary least squares multivariable regression models to identify demographic and clinical factors significantly associated with increasing WMH load in the whole SHIP sample ($n = 2367$). We considered the total WMH burden rather than the common distinction between periventricular and deep WMH, as these measures were highly correlated (DeCarli *et al.*, 2005). Two models were built separately for all participants in this study to assess relationships between the risk factors and the increasing WMH volume and count (i.e. discretizing the WMH into single lesions and then summing them up). Since WMH volume is a right-skewed measure, we considered a simple cubic root transformation to normalize the distribution in the regression models and increase the statistical power. Furthermore, we investigated whether the risk factors have similar association with WMH volume and count after exclusion of possibly impaired individuals according to their age-adjusted cognitive scores ($n = 232$) as a supplementary analysis.

To study the relationship between grey matter atrophy related to high WMH burden and brain ageing, we focused on SHIP subjects $\geqslant 40$ years, as the prevalence of WMH starts to increase after this age. WMH is a highly skewed measure with a large variability for subjects with low values. For this reason, instead of applying a regression type of analysis using continuous values, we focused on the extremes of the distribution, by identifying subjects with high and low WMH burden, to capture the most discriminative patterns associated with WMH. Selection of high and low WMH burden subjects is done independently in two age categories: (i) middle age from 40 to 65 years in which WMH start to appear increasingly with age; and (ii) old age $\geqslant 65$ years, as the exponential increase of Alzheimer's disease prevalence starts from this age. In each age category, we modelled the relationship between age as independent variable and WMH volume as dependent variable in a quantile regression approach. We defined, in each age category, the high WMH burden individuals as above the 80th percentile of WMH volume as a function of age and low individuals as below the 20th percentile.

To identify subjects with advanced and resilient to brain age, we modelled the relationship between age as independent variable and SPARE-BA as dependent variable in a linear regression approach. Residuals were transformed with z-score transformation. Subjects with z-score $> 0.5$ were grouped as resilient to brain ageing and those below $-0.5$ as advanced brain ageing (Supplementary Fig. 2).

We performed statistical group comparisons using on optimal-discriminative voxel-based analysis (Zhang and Davatzikos, 2011, 2013; Erus *et al.*, 2014) (ODVBA) on the grey matter RAVENS maps to detect spatial patterns of regional volumetric differences between high and low WMH

load groups. A similar analysis was performed independently to detect significant imaging patterns that differentiate between advanced and resilient to brain ageing groups. Final statistical maps of group differences were corrected using the false discovery rate correction and values are reported at a significance level of $q < 0.05$.

To study the mediation effect of cardiovascular disease risk score (CVD-RS) and WMH volume (both jointly and separately) on individual brain ageing we performed mediation analysis using structural equation modelling, which recently showed significant mediation effects on age-related differences in a cross-sectional ageing study (Kievit *et al.*, 2014). We used the technique implemented in the lavaan, an R package, (https://cran.r-project.org/web/packages/lavaan/index.html) for latent variable analysis including structural equation modelling (Rosseel, 2012). We modelled the SPARE-BA index as dependent variable, age as independent variable as well as CVD-RS and WMH volume as mediators. We independently constructed a similar model with the SPARE-AD index as the dependent variable. Analyses and graphics were performed using R software (v3.0) (Team RDC, 2008).

# Results

## Prevalence of WMH in the general population

Figure 1 shows the WMH volume plotted as a function of age for each individual of SHIP included in this study ($n = 2367$). In general, WMH volumes larger than 2000 $mm^3$ started to appear after the fifth decade of life, and became increasingly larger for subjects $\geqslant 65$ years. The Spearman's rank correlation coefficient between increasing WMH volume and age was 0.58 ($P < 0.0001$) for the whole SHIP sample. Age in turn had a Spearman's rank correlation coefficient of $-0.80$ and 0.38 ($P < 0.0001$) with SPARE-BA and SPARE-AD, respectively.

Figure 2 shows the SHIP subjects in middle (40–65 years) and old ages ($>65$ years) divided in two groups: high ($n = 282$ middle age, $n = 102$ old age) and low WMH burden ($n = 282$ middle age, $n = 101$ old age) groups, respectively as well as the group corresponding SPARE-BA index as function of age. Mean SPARE-BA and SPARE-AD of the high WMH group were significantly different compared to the mean SPARE-BA and SPARE-AD of the low WMH group in the middle and old age categories (Supplementary Table 2).

In Fig. 3 we show lesion frequency maps of subjects in the high WMH group for each age category. The figure shows a clear pattern of lesions that accumulate from periventricular areas in middle age (40–65 years, $n = 282$) to more pronounced and frequent periventricular lesions with larger spatial extend and deep white matter frontal lobe lesions in old age ($>65$ years, $n = 102$). The lesion frequency maps for the whole SHIP sample for every decade, starting from the fifth one, are presented in Supplementary Fig. 3.

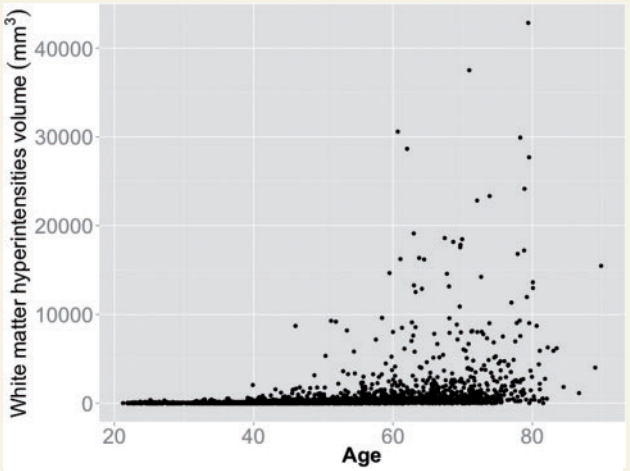


**Figure 1 WMH volume as function of age for the whole SHIP sample included in this study ($n = 2367$).**

## Risk factors associated with WMH volume

Multivariable regression models revealed significant associations between age, gender, hypertension, diabetes mellitus, smoking and education level and increased WMH volume and count (Table 2). In Supplementary Table 3 the associations of those risk factors with increased WMH volume and count are reported after exclusion of possibly impaired individuals based on low age adjusted cognitive scores ($n = 234$), which lead to similar results. In Supplementary Table 4 the associations of those risk factors with increased WMH volume and count are reported after considering the internal carotid stenosis variable as an additional risk factor, which also leads to similar results. The association between WMH volume and the CVD-RS was significant ($P = 0.003$) after adjusting for age, gender and education in a linear regression model in the full SHIP sample of this study.

## Association with cognitive scores

WMH volume was significantly associated with the immediate recall of the verbal learning and memory test subscore for SHIP-2 ($n = 730$), but the delayed recall was not. With Nurnberg age inventory subscores there was no significant association for SHIP-Trend ($n = 1637$) after adjusting for age, education and gender in linear regression approaches. The results are represented in Supplementary Table 5.

## Association with the presence of *APOE* $\varepsilon 4$

No significant association was detected between WMH volume or count and the presence of at least one *APOE* $\epsilon 4$ allele in the SHIP sample with available *APOE* genotyping ($n = 1472$).

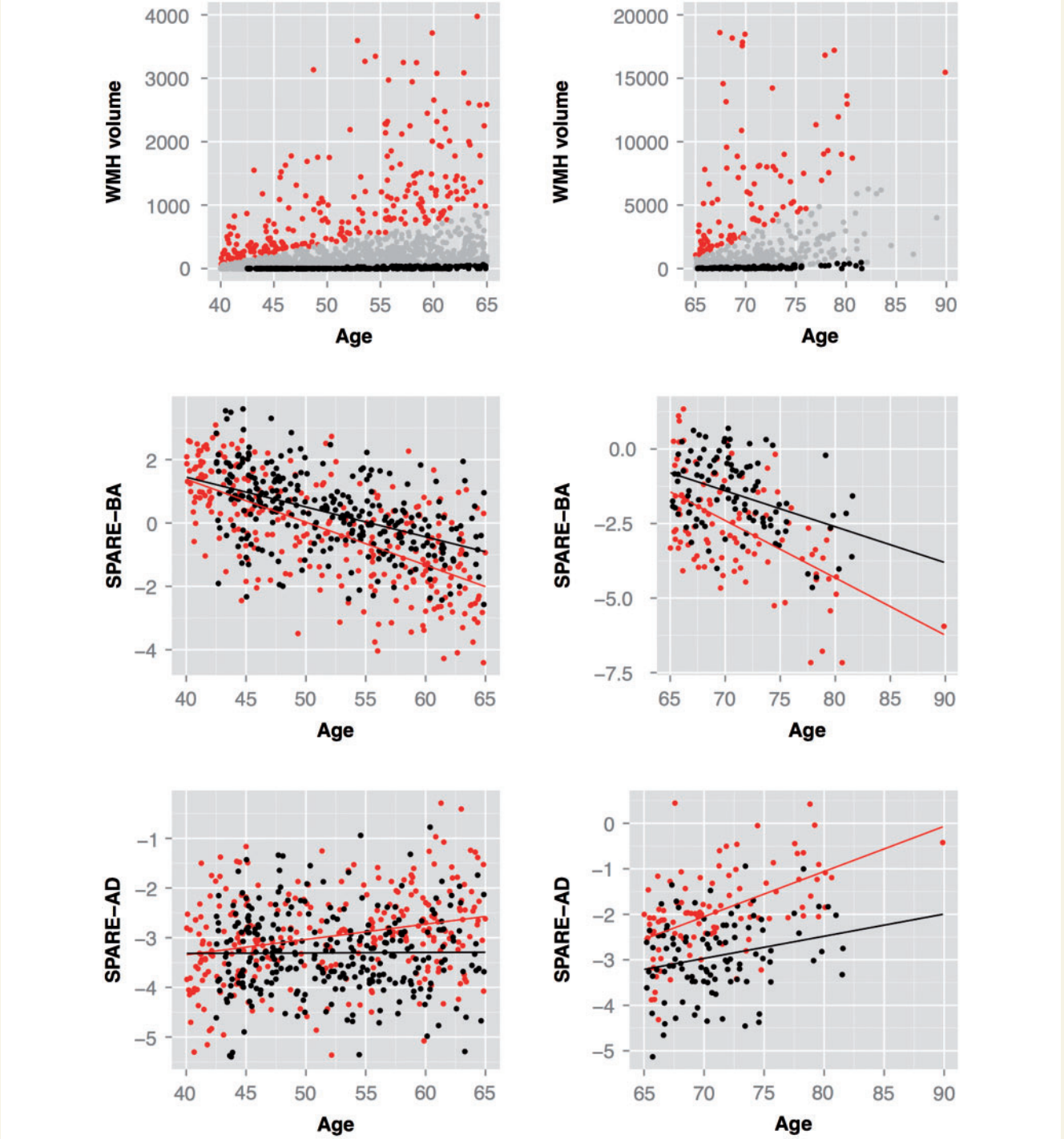


**Figure 2 SHIP individuals with high and low WMH burden and the corresponding SPARE indices.** *Top row*: WMH volume for SHIP subjects in middle (40–65 years old) and old (>65 years old) age categories. Based upon WMH volume, we grouped these subjects into subjects with high WMH load (red dots; above the 80th percentile of WMH volume as a function of age, $n$ = 282 for middle and $n$ = 102 for old ages) and low WMH load (black dots; below the 20th percentile of WMH volume as a function of age, $n$ = 282 for middle and $n$ = 101 for old ages). *Middle row:* The relationship between age and SPARE-BA (reflecting ageing patterns of brain atrophy) in both groups. *Bottom row:* The relationship between age and SPARE-AD (capturing patterns of atrophy in Alzheimer's disease-related regions) in both groups. Individuals with high WMH load have higher SPARE-AD and lower SPARE-BA values ($P < 0.0001$).

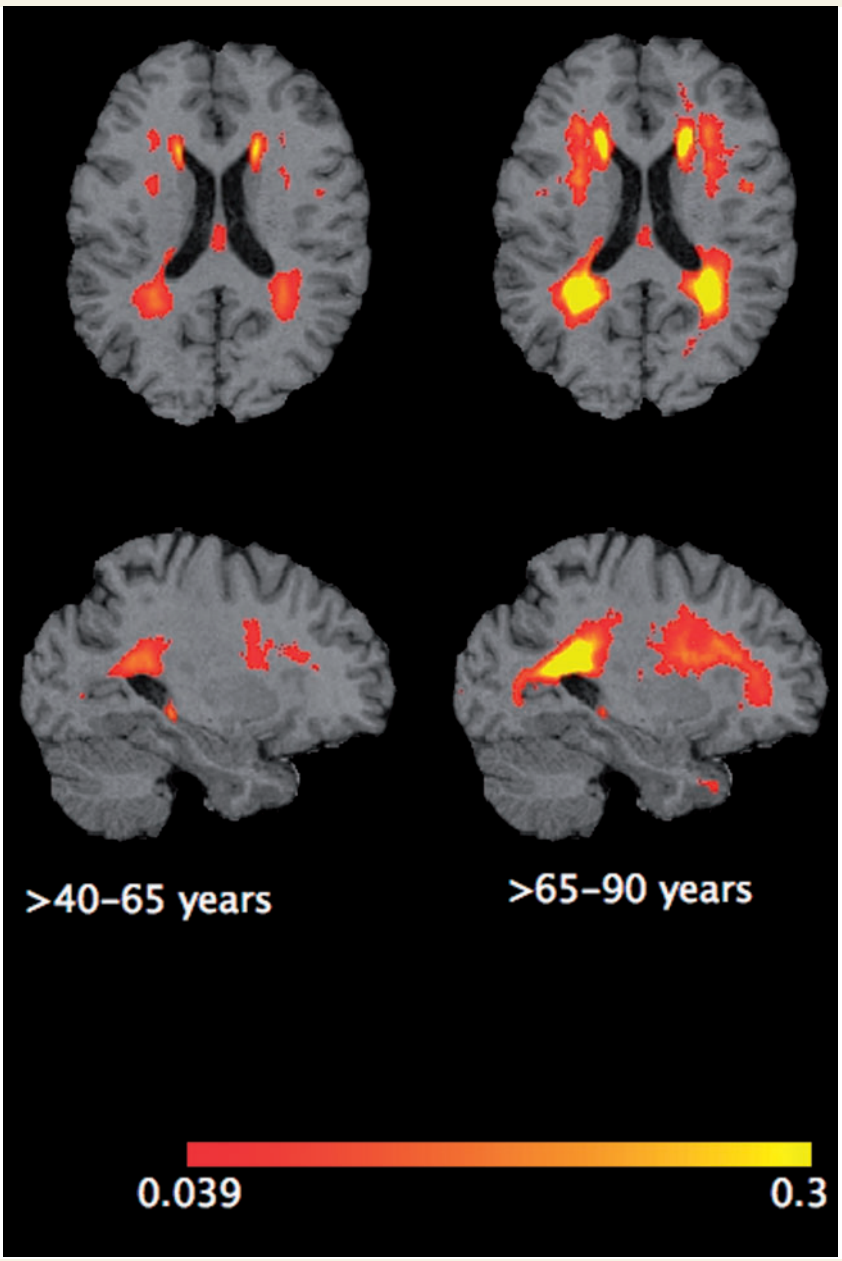


**Figure 3 Frequency maps of WMH in the high burden groups in middle ($n$ = 282), and old ($n$ = 102) age categories.** *Upper* row presents axial view and the *lower*, sagittal view.

## Mediation of age effect through WMH and CVD-RS on the SPARE-BA index

Figure 4 shows the model developed in this study to understand the mediation of age effect through CVD-RS and WMH on SPARE-BA. The model shows that the complete mediation effect of age through WMH and CVD-RS explains 29.8% of the variance of SPARE-BA. While 10.4% of the variance of SPARE-BA can be explained by WMH mediating age, CVD-RS explains 21.6% of it. The mediation proportion of age through CVD-RS that is exclusively mediated by WMH was 2.3%. All results were statistically significant ($P < 0.0001$). Supplementary Table 6 presents the complete parameters related to this mediation model.

## Mediation of age effect through WMH and CVD-RS on the SPARE-AD index

Figure 5 shows the model developed in this study to understand the mediation of age effect through CVD-RS and WMH on SPARE-AD. The model shows that the complete mediation of age effect through WMH and CVD-RS explains

**Table 2 Multiple regression models for WMH volume and count in the whole SHIP sample included in this study ($n$ = 2367)**

| Factor | $\sqrt[3]{\text{WMH}}$ volume All participants ⩾20 years $n$ = 2367 | | | WMH count All participants ⩾20 years $n$ = 2367 | | |
|---|---|---|---|---|---|---|
| | Estimate | SE | $P$-value (factor) | Estimate | SE | $P$-value (factor) |
| **Gender, female** | −0.695 | 0.265 | **0.008*** | −0.694 | 0.281 | **0.013*** |
| **Age, years** | 0.183 | 0.008 | **<0.0001*** | 0.159 | 0.009 | **<0.0001*** |
| **Systolic blood pressure, mmHg** | 0.020 | 0.005 | **0.001*** | 0.014 | 0.006 | **0.012*** |
| **Cholesterol ratio (high-density lipoprotein/low-density lipoprotein)** | 0.476 | 0.445 | 0.284 | 0.668 | 0.472 | 0.157 |
| **Glycated haemoglobin (HbA1c), %** | −0.127 | 0.133 | 0.340 | −0.080 | 0.141 | 0.568 |
| **Cigarette smoking** | | | | | | |
| Ex-smoker | 0.588 | 0.193 | **0.002*** | 0.649 | 0.205 | **0.001*** |
| Current smoker | 0.623 | 0.232 | **0.007*** | 0.607 | 0.246 | **0.013*** |
| **Waist circumference, cm** | −0.005 | 0.009 | 0.548 | −0.001 | 0.009 | 0.975 |
| **Education** | | | | | | |
| 8–10 years | −0.767 | 0.262 | **0.003*** | −0.657 | 0.278 | **0.018*** |
| >10 years | −0.529 | 0.285 | 0.063 | −0.459 | 0.302 | 0.129 |
| **Physical activity** | | | | | | |
| No sport related activity | 0.004 | 0.231 | 0.982 | 0.132 | 0.245 | 0.589 |
| >0–1 h/week | −0.129 | 0.275 | 0.637 | −0.281 | 0.292 | 0.335 |
| >1–2 h/week | 0.022 | 0.232 | 0.921 | −0.056 | 0.246 | 0.820 |
| **Body height, cm** | 0.008 | 0.013 | 0.532 | 0.007 | 0.014 | 0.588 |
| **Antihypertensive drugs** | 0.395 | 0.214 | 0.065 | 0.614 | 0.227 | **0.007*** |
| **Antidiabetic drugs** | 1.089 | 0.479 | **0.023*** | 0.680 | 0.509 | 0.181 |
| **Lipid lowering drugs** | 0.187 | 0.308 | 0.542 | −0.199 | 0.326 | 0.541 |
| | | $R^2$ = 0.333 | | | $R^2$ = 0.254 | |

*Significance at level $P < 0.05$.
SE = standard error.

33.9% of the variance of SPARE-AD. While 32.8% of the variance of SPARE-AD can be explained by WMH mediating age, CVD-RS explains 8.4% of it. The mediation proportion of age through CVD-RS that is exclusively mediated by WMH was 7.2%. Supplementary Table 7 presents the complete parameters related to this mediation model

## Grey matter atrophy patterns related to high WMH

Figure 6 shows regions where the high WMH group showed less grey matter compared to low WMH subjects in middle and old ages. Supplementary Fig. 4 shows brain sections resulted from the ODVBA comparison showing hippocampal involvement. Significant grey matter atrophy was mainly present in the parietal and temporal lobes during middle age and more in the frontal, parietal and temporal lobes during older age. Most notable was the larger frontal lobe atrophy in older subjects. Figure 6 illustrates the spatial patterns of regional volumetric differences between resilient and advanced brain ageing groups (in blue) and between low and high WMH load groups (in orange) as well as the overlap between both (in green). Supplementary Tables 8 and 9 provide complete significant regions statistics for group comparison between high versus low WMH groups and Supplementary Tables 10 and 11 provide complete significant regions statistics between resilient versus advanced brain ageing groups.

# Discussion

The current study expands upon previous studies that have shown an association between age and WMH, by quantitatively analysing the relationship between WMH and the spatial distribution of brain atrophy in a large neuroimaging sample from the adult general population. Utilizing machine learning techniques, we used two indices to quantify atrophy patterns: SPARE-BA measured age-related patterns; and SPARE-AD measured patterns of brain atrophy found in Alzheimer's disease patients. We found that individuals with high WMH burden display spatial patterns of atrophy that partially overlap with advanced brain ageing, which was defined as deviation from normal age-related

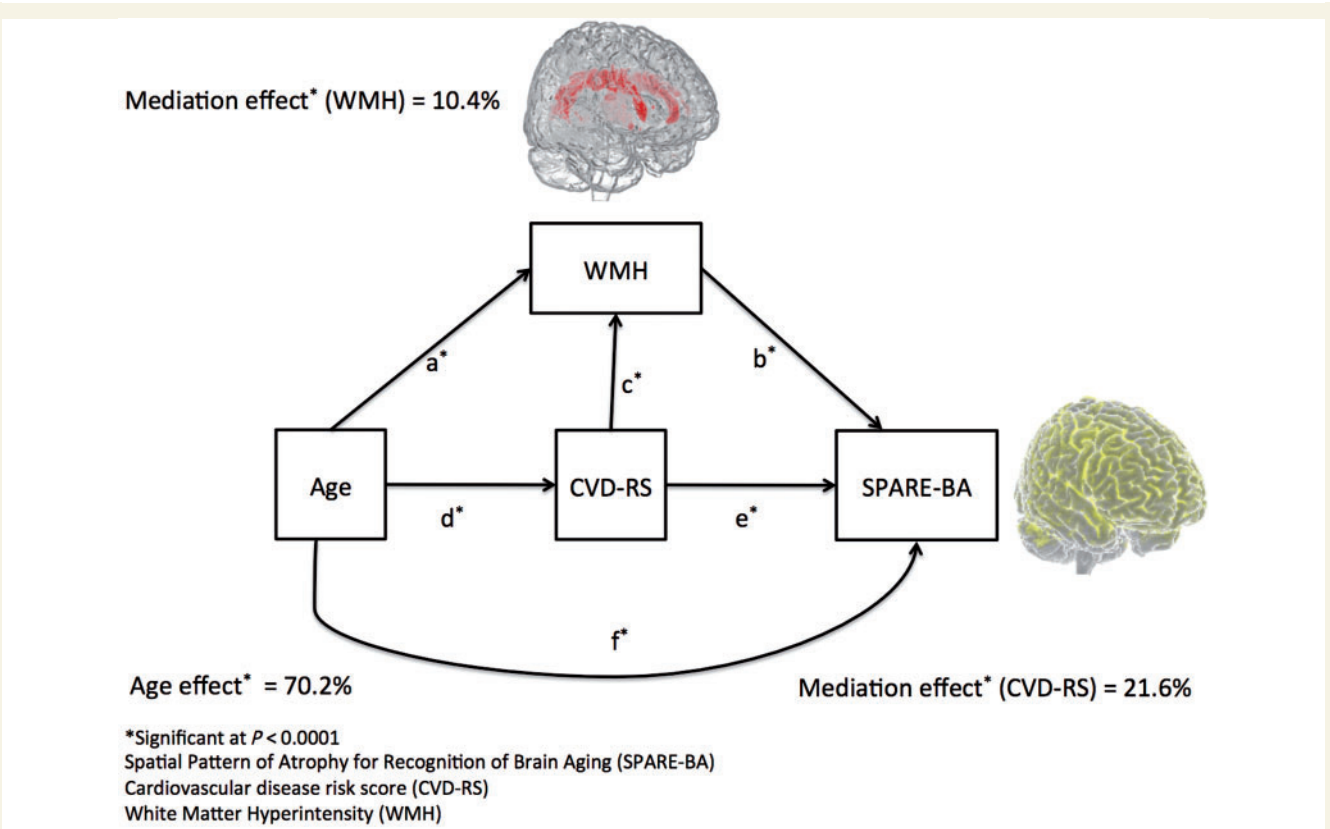


**Figure 4 Path diagram of the factors associated with the SPARE-BA index.** WMH had 10.4% [95% confidence interval (CI): 8.4–12.4%] mediation of age effect on the SPARE-BA index (paths ab and dcb). CVD-RS had a 21.6% (95% CI: 17.4–25.7%) mediation of age effect on the SPARE-BA index (paths de and dcb). The common path through CVD and WMH (path dcb) shows 2.3% (95% CI: 1.3–3.3%) mediation of age effect on brain atrophy. The total mediation of age effect through WMH and CVD-RS together (path ab, dcb and de) was 28.9 (95% CI: 25.4–34.1%). The direct age effect on SPARE-BA (path f) was 70.2% (95% CI: 65.9–74.6%). All results were statistically significant ($P < 0.0001$).

patterns of brain change captured by SPARE-BA. Additionally, high WMH were associated with higher SPARE-AD values in the general population.

## WMH and associations with risk factors

A recent systematic review provides a comprehensive overview of risk factor associations with WMH (Grueter and Schulz, 2012). The large sample size of our study enabled analyses of risk factors in relation to WMH. Our findings of more WMH in smokers are consistent with prior reports demonstrating an increase in WMH volume compared with non-smokers (Jeerakathil *et al.*, 2004). We also observed that anti-hypertensive medication use was associated with more WMH volume. Anti-hypertensive medication could be considered a proxy for chronic and poorly regulated hypertension, and thus, our findings are consistent with prior reports that hypertension is associated with increasing WMH (Longstreth *et al.*, 1996; Jeerakathil *et al.*, 2004). Our observations of more WMH in diabetic individuals compared to those without diabetes mellitus are in line with a prior report indicating a similar association in a smaller sample (Jongen *et al.*, 2007). Furthermore, our results show a significant negative association between WMH and level of education, which may be explained in terms of different socio-economic status between high and low educated individuals and is in line with a previous study that reported a significant association between income and WMH (Longstreth *et al.*, 1996). Previous studies showed associations between cognitive impairment and WMH (Prins and Scheltens, 2015) and one related this decline to grey matter atrophy rather than WMH (Schmidt *et al.*, 2005). However, our results showed only significant negative association between the immediate recall score of the verbal learning and memory test and increased WMH volume. Even with the rather limited cognitive assessment in SHIP we could observe partial association with cognitive performance. A previous study showed no significant association between large-artery atheromatous disease and WMH (Wardlaw *et al.*, 2014), in line with our results for WMH volume. However our sample included a low number of participants with clinically relevant stenosis in the left or right internal carotid artery (<0.02%) and therefore further studies should be conducted.

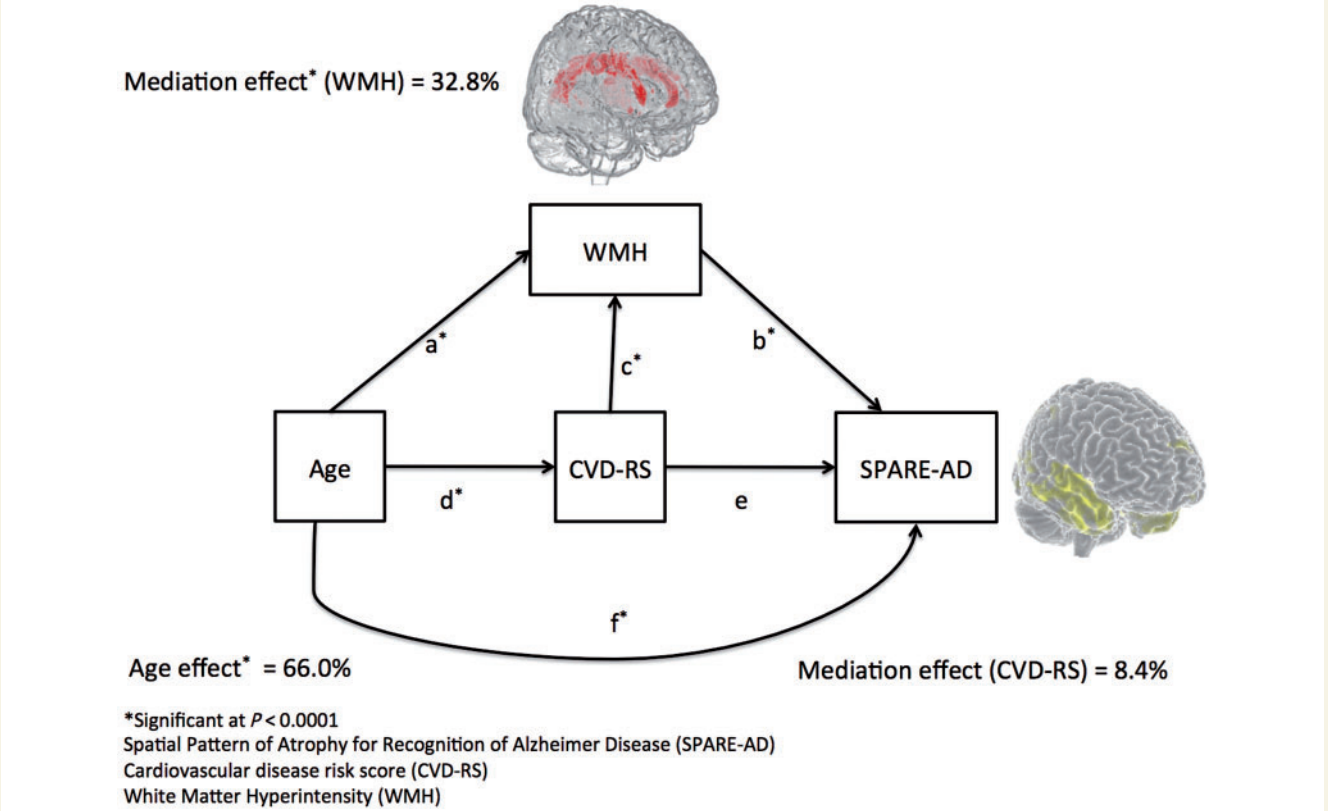


**Figure 5 Path diagram of the factors associated the SPARE-AD index.** WMH had 32.8% (95% CI: 25.6–40.3%) mediation of age effect on the SPARE-AD index (paths ab and dcb). CVD-RS had 8.4% (95% CI: −6–23.1%) mediation of age effect on the SPARE-AD index (paths de and dcb). The common path through CVD and WMH (path dcb) shows 7.3% (95% CI: 4.4–10.8%) mediation of age effect on brain atrophy. The total mediation of age effect through WMH and CVD-RS together (path ab, dcb and de) was 34.0% (95% CI: 18.7–50.1%). The direct age effect on SPARE-AD (path f) was 66.0% (95% CI: 49.9–81.2%).

## Association with *APOE* genotype

The results for the association between *APOE* genotype and WMH are controversial (Prins and Scheltens, 2015). Our results showed no association between the presence of at least one *APOE* $\epsilon$4 allele and WMH in SHIP. Interestingly, a recent genome-wide association study reported that novel loci contained genes significantly associated with WMH volume that have been implicated in Alzheimer's disease (Verhaaren *et al.*, 2015).

## The mediation effect of WMH and CVD-RS on SPARE-BA and SPARE-AD

Several mechanisms have been proposed to explain the association between WMH and grey matter atrophy, such as ischaemic damage (Du *et al.*, 2005) or Wallerian degeneration (Erten-Lyons *et al.*, 2013). Cardiovascular disease risk factors in turn increase the risk of atherosclerosis that might lead to decreased blood flow in the grey matter and consequently to more brain ageing patterns (Dai *et al.*, 2008; Moran *et al.*, 2013). In fact vascular pathology and axonal loss are both present in ageing brains and this can explain the association between brain ageing patterns and the presence of WMH.

Erten-Lyons *et al.* (2013) suggested two possibilities for the link between Alzheimer's disease pathology and WMH first due to Wallerian degeneration secondary to neurodegenerative changes, second due to ischaemic injury to the axons, manifested as white matter changes, which may lead to tangle formation and neuronal degeneration. Ihara *et al.* (2010) suggested an effect for demyelination in the cases with Alzheimer's disease and dementia with Lewy bodies combined, which in turn could be responsible for the appearance of WMH. In other words, there is a possibility that neurodegenerative changes secondarily induce WMH. Although our study confirms a strong relationship between WMH and SPARE-BA and SPARE-AD patterns of atrophy in the general adult population, it cannot reveal the underlying biological mechanisms that lead to this relationship.

Wardlaw *et al.* (2014) reported that WMH have a large non-vascular, non-atheromatous aetiology. We showed that the proportion of WMH variance explained by CVD-RS was only 25.2% (Supplementary Table 12). While this value is small, and thus suggests that WMH cannot be

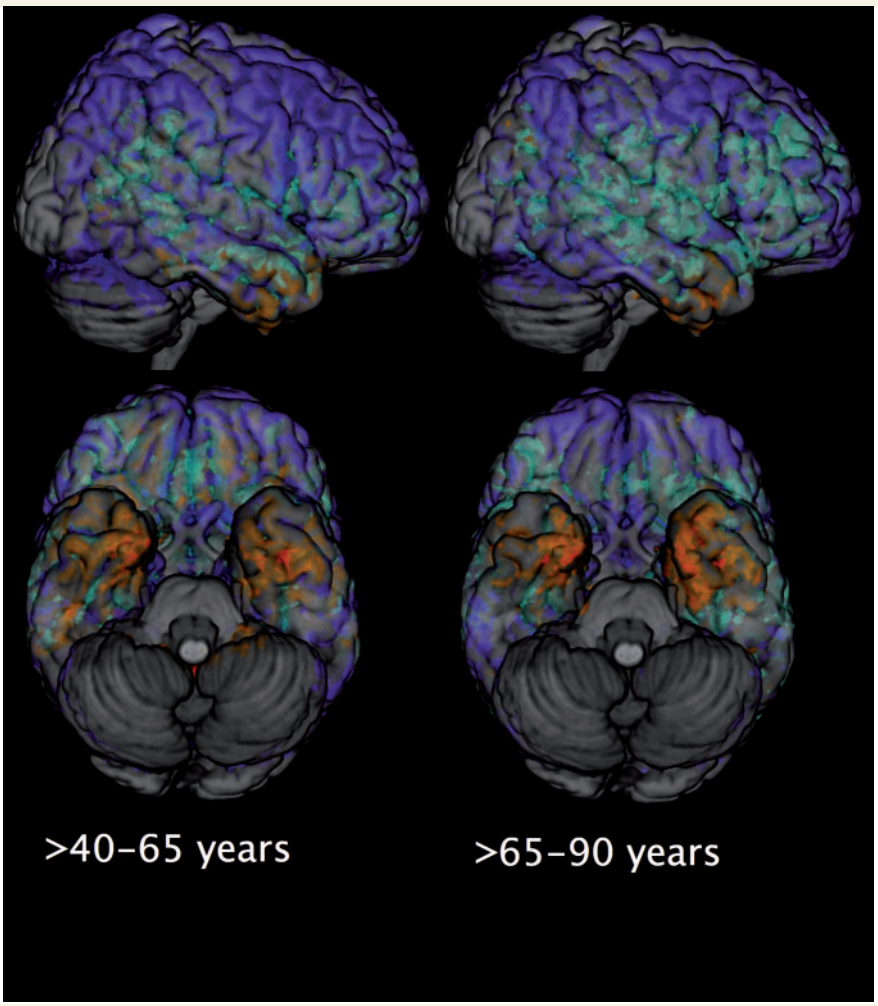


**Figure 6 Regions of significant group differences in gray matter atrophy between individuals with high and low WMH burden in relation to advanced brain aging patterns of atrophy.** Blue: regions displaying significant regional atrophy patterns between resilient ($n$ = 439 middle age, $n$ = 167 old age) and advanced brain ageing ($n$ = 393 middle age, $n$ = 158 old age) individuals. Orange: regions displaying significant WMH-related patterns of atrophy in high ($n$ = 282 middle age, $n$ =102 old age) versus low WMH ($n$ = 282 middle age, $n$ = 101 old age) individuals. Green: overlap of the blue and orange regions (false discovery rate correction with $q < 0.05$).

explained uniquely by vascular factors, it is larger than the 2% reported by Wardlaw *et al.* (2014). We believe that this difference may be related to differences in sample demographics: while their study had subjects with similar age, our study population was sampled from the general population with a wide age range (20–90 years), which gives large age effect within the explained variance from vascular origin.

## Spatial patterns of grey matter atrophy related to high WMH burden

Recent studies have shown possible relationships between WMH and global grey matter atrophy reduction and WMH (Aribisala *et al.*, 2013; Wang *et al.*, 2014), atrophy in the medial temporal (Appel *et al.*, 2009), temporal (Wen *et al.*, 2006; Tuladhar *et al.*, 2015), and the frontal cortex (Raji *et al.*, 2012), bilateral hippocampus (Crane *et al.*, 2015) and in the superior parieto-occipital cortex (Smith *et al.*, 2015).

We found significant grey matter regional atrophy in brains with high WMH burden compared to those with low WMH burden, which survived false discovery rate correction. This difference was mainly present in the temporal lobe as the centre of the affected region in the middle age group, expanding later in life to more frontal cortex (Fig. 6). Further regions include anterior temporal lobe and inferior frontal cortex, hippocampus, parahippocampal gyrus, insula, amygdala and cingulate (Supplementary Fig. 4 and Supplementary Tables 8 and 9).

This pattern of deposition in the anterior temporal and inferior frontal cortex may seem somewhat unusual for WMH. Tullberg *et al.* (2004) showed that, regardless of their regional distribution, WMH were associated with metabolic effects on the frontal lobes. These effects were more prominent in non-demented subjects with strong

effects on executive function. More specific were Raz *et al.* (2008) in showing that vascular risk was associated with smaller prefrontal volumes. The anterior temporal lobe in turn has dense connectivity with a number of sensory modalities e.g. white matter tracts have been observed between the anterior temporal lobe and the frontal lobe via the uncinate fasciculate (Kubicki *et al.*, 2002).

Our results showed that individuals with high WMH burden have higher SPARE-AD values. Higher SPARE-AD values indicate the presence of more atrophy in Alzheimer's disease-related regions, albeit this atrophy might not be specific for Alzheimer's disease and might be present in other types of dementia. Our ODVBA results showed that high WMH burden is associated with atrophy in regions associated with age-related atrophy in previous work; amygdala, prefrontal, cerebellum and cingulate cortex (Draganski *et al.*, 2011). Our results suggest that the regions of relatively more pronounced brain atrophy found in individuals with high WMH burden overlapped substantially, but only partially with the advanced brain ageing-related patterns (Fig. 6, in green) mainly in parts of the temporal lobe as well as frontal lobe, especially in the old age category (>65 years). The association between WMH and brain ageing-related atrophy has been confirmed in our analysis with SPARE-BA. Individuals with high WMH burden had lower SPARE-BA values compared to individuals with low WMH burden, which is associated with more ageing atrophy (Fig. 2). Advanced brain ageing patterns were widespread in the brain (Fig. 6, in blue), but interestingly WMH-related patterns of atrophy were unique in orbitofrontal, anterior, medial and inferior temporal regions (Fig. 6, in orange). Atrophy was observed in those regions in several dementia types such as Alzheimer's disease (Wang *et al.*, 2015), frontotemporal lobar degeneration, Lewy body disease (Vemuri *et al.*, 2011) and semantic dementia (Duval *et al.*, 2012). Additionally those regions are strongly associated with cognitive impairment in other work (Pennanen *et al.*, 2005; DeCarli *et al.*, 2007).

Using a longitudinal sample of prospectively followed subjects from the BLSA study, Davatzikos *et al.* (2009) examined the longitudinal progression of SPARE-AD, and displayed that the rate of longitudinal SPARE-AD change could distinguish between cognitively normal older adults who progressed to mild cognitive impairment and those who did not. Our data demonstrate that the SPARE-AD change due to WMH in Fig. 2 has pushed the participants about a decade or more along the SPARE-AD curve, derived from well characterized, prospectively studied normal controls in Davatzikos *et al.* (2009) (see their figure 4). Given that the SPARE-AD was a good predictor of conversion from normal to mild cognitive impairment, and from mild cognitive impairment to Alzheimer's disease, the SHIP results show that high WMH individuals have an atrophy in Alzheimer's disease dementia-related regions by about a decade, as seen from the brain structure angle. Previous neuropathological studies have also demonstrated the cumulative effect of vascular and Alzheimer's disease pathology on cognition (Petrovitch *et al.*, 2005; Toledo *et al.*, 2013). From a complementary perspective, Fig. 2 indicates that high-WMH individuals have brains that have more age atrophy for ~8 years, at age 55, and this difference increases thereafter.

While previous work has been conducted using region of interest-based analyses (Appel *et al.*, 2009; Aribisala *et al.*, 2013; Wang *et al.*, 2014), cortical thickness (Smith *et al.*, 2015; Tuladhar *et al.*, 2015) and voxel-based morphometry or related methods (Wen *et al.*, 2006; Raji *et al.*, 2012; Crane *et al.*, 2015), our study also used the SPARE-BA index to quantify the presence of spatial patterns of atrophy on an individual basis indicating that subjects who present relatively higher WMH burden tend to have beyond normal brain age-related atrophy.

## Strengths and limitations

This study has several strengths including the large sample size in a population-based community sample with highly standardized imaging and phenotyping and the use of pattern analysis methods, including the SPARE indices, ODVBA and mediation analysis, as well as automated WMH delineation. However, this study also has limitations: (i) the lack of serial magnetic resonance scans did not offer us the possibility to study longitudinal effects of WMH; (ii) we lacked the continuous description of some variables as they were categorically recorded (such as education and physical activity); (iii) the determination of *APOE* was based on genotyping and not following the clinical standards for *APOE* determination; (iv) the cognitive assessment in SHIP was limited, which renders it difficult to relate the observed patterns of brain atrophy with cognitive performance; (v) our SPARE-BA model has been trained with a sample from the general population, in which possible overlap between WMH and brain ageing risk factors is present (Debette *et al.*, 2011; Franke *et al.*, 2012; Gardener *et al.*, 2015). This in turn could lead to certain circularity in our results. Constructing a classifier with complete independence between WMH and brain ageing from any overlapping risk factors is a challenging task in a sample from the general population. An absolute healthy subsample could require deeper risk factor analysis (and some related risk factors might not be recorded in the SHIP database); (vi) while we show that individuals with high WMH burden have higher SPARE-AD scores, the atrophy patterns captured by the SPARE-AD model may not be specific in differentiating between dementia types, which cannot be done in the current study in the absence of any additional Alzheimer's disease-related marker in SHIP; (vii) the use of the distance in a binary support vector machine as an index should be done with caution. Given that we are using regional volumetric measures as input features for the classification, the SPARE scores represent brain volume changes in specific brain regions (as shown in Supplementary Fig. 5). However, the score

remains hinged on the training set. For SPARE-BA we used a training set from the same study (SHIP). On the other hand there were no demented participants in SHIP; therefore we used a training model from a different study previously derived in Da *et al.* (2014). For this reason, for the SPARE-AD score, the distance from the hyperplane might be less generalizable, although previous studies showed good generalization power (Davatzikos *et al.*, 2009); (viii) some modifiable risk factors such as dietary factors (e.g. salt or sugar intake) and inflammation were not included in the study; and (ix) finally, our analysis did not include infarcts and periventricular spaces assessment and those should be considered in future research.

# Conclusion

Our study indicates that high WMH load is associated with grey matter atrophy overlapping with advanced brain ageing. Furthermore, CVD-RS and WMH significantly mediate the effect of age on cortical grey matter atrophy. Considering those effects: CVD risk factors and WMH may constitute a dual hit (of two very common conditions) that accelerates the clinical manifestation and progression of neurodegeneration in the general population. Furthermore, preventive strategies reducing the odds to develop CVD and WMH (Gorelick *et al.*, 2011) could decrease the incidence or delay the onset of dementia.

# Funding

SHIP is part of the Community Medicine Research net of the University of Greifswald, Germany, which is funded by the Federal Ministry of Education and Research (grants no. 01ZZ9603, 01ZZ0103, and 01ZZ0403), the Ministry of Cultural Affairs and the Social Ministry of the Federal State of Mecklenburg-West Pomerania. Genome-wide data in SHIP and MRI scans in SHIP and SHIP-TREND have been supported by a joint grant from Siemens Healthcare, Erlangen, Germany and the Federal State of Mecklenburg-West Pomerania. Genome-wide genotyping in SHIP-TREND-0 was supported by the Federal Ministry of Education and Research (grant no. 03ZIK012). This work was supported in part by NIH grant R01-AG14971. S.V.A. was supported by the German Federal Ministry of Education and Research (BMBF) within the framework of the e:Med research and funding concept (Integrament; grant no. 01ZX1314E). J.B.T. is supported by P01 AG032953, PO1 AG017586, P30 AG010124 and P50 NS053488. M.H. was supported by '*Alfried Krupp von Bohlen und Halbach*' foundation. No conflict of interest to be declared.

# Supplementary material

Supplementary material is available at *Brain* online.

# References

Appel J, Potter E, Bhatia N, Shen Q, Zhao W, Greig MT, et al. Association of white matter hyperintensity measurements on brain MR imaging with cognitive status, medial temporal atrophy, and cardiovascular risk factors. Am J Neuroradiol 2009; 30: 1870–6.

Aribisala B, Valdés Hernández M, Royle N, Morris Z, Muñoz Maniega S, Bastin M, et al. Brain atrophy associations with white matter lesions in the ageing brain: the Lothian Birth Cohort 1936. Eur. Radiol 2013; 23: 1084–92.

Brickman AM, Zahodne LB, Guzman VA, Narkhede A, Meier IB, Griffith EY, et al. Reconsidering harbingers of dementia: progression of parietal lobe white matter hyperintensities predicts Alzheimer's disease incidence. Neurobiol Aging 2015; 36: 27–32.

Carmichael O, Schwarz C, Drucker D, Fletcher E, Harvey D, Beckett L, et al. Longitudinal changes in white matter disease and cognition in the first year of the alzheimer disease neuroimaging initiative. Arch Neurol 2010; 67: 1370–8.

Coker LH, Hogan PE, Bryan NR, Kuller LH, Margolis KL, Bettermann K, et al. Postmenopausal hormone therapy and subclinical cerebrovascular disease: the WHIMS-MRI Study. Neurology 2009; 72: 125–34.

Crane DE, Black SE, Ganda A, Mikulis DJ, Nestor SM, Donahue MJ, et al. Gray matter blood flow and volume are reduced in association with white matter hyperintensity lesion burden: a cross-sectional MRI study. Front Aging Neurosci 2015; 7: 131.

D'Agostino RB, Vasan RS, Pencina MJ, Wolf PA, Cobain M, Massaro JM, et al. General cardiovascular risk profile for use in primary care: the framingham heart study. Circulation 2008; 117: 743–53.

Dai W, Lopez OL, Carmichael OT, Becker JT, Kuller LH, Gach HM. Abnormal regional cerebral blood flow in cognitively normal elderly subjects with hypertension. Stroke 2008; 39: 349–54.

Davatzikos C, Genc A, Xu D, Resnick SM. Voxel-based morphometry using the RAVENS maps: methods and validation using simulated longitudinal atrophy. Neuroimage 2001; 14: 1361–9.

Davatzikos C, Xu F, An Y, Fan Y, Resnick SM. Longitudinal progression of Alzheimer's-like patterns of atrophy in normal older adults: the SPARE-AD index. Brain 2009; 132: 2026–35.

Da X, Toledo JB, Zee J, Wolk DA, Xie SX, Ou Y, et al. Integration and relative value of biomarkers for prediction of MCI to AD progression: Spatial patterns of brain atrophy, cognitive scores, APOE genotype and CSF biomarkers. Neuroimage Clin 2014; 4: 164–73.

Debette S, Seshadri S, Beiser A, Au R, Himali J, Palumbo C, et al. Midlife vascular risk factor exposure accelerates structural brain aging and cognitive decline. Neurology 2011; 77: 461–8.

DeCarli C, Fletcher E, Ramey V, Harvey D, Jagust WJ. Anatomical mapping of white matter hyperintensities (WMH): exploring the relationships between periventricular WMH, Deep WMH, and total WMH burden. Stroke 2005; 36: 50–5.

DeCarli C, Frisoni GB, Clark CM, Harvey D, Grundman M, Petersen RC, et al. Qualitative estimates of medial temporal atrophy as a predictor of progression from mild cognitive impairment to dementia. Arch Neurol 2007; 64: 108–15.

Dickerson BC, Bakkour A, Salat DH, Feczko E, Pacheco J, Greve DN, et al. The cortical signature of Alzheimer's disease: regionally specific cortical thinning relates to symptom severity in very mild to mild AD dementia and is detectable in asymptomatic amyloid-positive individuals. Cereb Cortex 2009; 19: 497–510.

Doshi J, Erus G, Ou Y, Gaonkar B, Davatzikos C. Multi-atlas skull-stripping. Acad Radiol 2013; 20: 1566–76.

Draganski B, Ashburner J, Hutton C, Kherif F, Frackowiak RSJ, Helms G, et al. Regional specificity of MRI contrast parameter changes in normal ageing revealed by voxel-based quantification (VBQ). Neuroimage 2011; 55: 1423–34.

Du A-T, Schuff N, Chao LL, Kornak J, Ezekiel F, Jagust WJ, et al. White matter lesions are associated with cortical atrophy more than entorhinal and hippocampal atrophy. Neurobiol Aging 2005; 26: 553–9.

Dufouil C, de Kersaint-Gilly A, Besancon V, Levy C, Auffray E, Brunnereau L, et al. Longitudinal study of blood pressure and white matter hyperintensities: the EVA MRI Cohort. Neurology 2001; 56: 921–6.

Duval C, Bejanin A, Piolino P, Laisney M, de La Sayette V, Belliard S, et al. Theory of mind impairments in patients with semantic dementia. Brain J Neurol 2012; 135: 228–41.

Erten-Lyons D, Woltjer R, Kaye J, Mattek N, Dodge HH, Green S, et al. Neuropathologic basis of white matter hyperintensity accumulation with advanced age. Neurology 2013; 81: 977–83.

Erus G, Battapady H, Zhang T, Lovato J, Miller ME, Williamson JD, et al. Spatial patterns of structural brain changes in type 2 diabetic patients and their longitudinal progression with intensive control of blood glucose. Diabetes Care 2014; 38: 97–9104.

Fan Y, Batmanghelich N, Clark CM, Davatzikos C, Alzheimer's Disease Neuroimaging Initiative. Spatial patterns of brain atrophy in MCI patients, identified via high-dimensional pattern classification, predict subsequent cognitive decline. Neuroimage 2008; 39: 1731–43.

Fan Y, Shen D, Gur RC, Gur RE, Davatzikos C. COMPARE: classification of morphological patterns using adaptive regional elements. IEEE Trans Med Imaging 2007; 26: 93–105.

Fleischmann UM, Oswald WD. Nürnberger-Alters-Inventar: (NAI): Testmanual und Textband. Göttingen, Germany: Hogrefe, Verlag für Psychologie. 1999.

Franke K, Gaser C, Manor B, Novak V. Advanced brainAGE in older adults with type 2 diabetes mellitus [Internet]. Front Aging Neurosci 2012; 5: 90. Available from: http://dx.doi.org/10.3389/fnagi.2013.00090

Franke K, Ziegler G, Klöppel S, Gaser C. Estimating the age of healthy subjects from T1-weighted MRI scans using kernel methods: Exploring the influence of various parameters. Neuroimage 2010; 50: 883–92.

Frisoni GB, Fox NC, Jack CR, Scheltens P, Thompson PM. The clinical use of structural MRI in Alzheimer disease. Nat Rev Neurol 2010; 6: 67–77.

Gardener H, Wright CB, Rundek T, Sacco RL. Brain health and shared risk factors for dementia and stroke. Nat Rev Neurol 2015; 11: 651–7.

Gaser C, Franke K, Klöppel S, Koutsouleris N, Sauer H, Initiative ADN. BrainAGE in mild cognitive impaired patients: predicting the conversion to Alzheimer's disease. PLoS One 2013; 8: e67346

Good CD, Scahill RI, Fox NC, Ashburner J, Friston KJ, Chan D, et al. Automatic differentiation of anatomical patterns in the human brain: validation with studies of degenerative dementias. Neuroimage 2002; 17: 29–46.

Gorelick PB, Scuteri A, Black SE, DeCarli C, Greenberg SM, Iadecola C, et al. Vascular contributions to cognitive impairment and dementia: a statement for healthcare professionals from the American Heart Association/American Stroke Association. Stroke 2011; 42: 2672–713.

Gouw AA, Seewann A, van der Flier WM, Barkhof F, Rozemuller AM, Scheltens P, et al. Heterogeneity of small vessel disease: a systematic review of MRI and histopathology correlations. J Neurol Neurosurg Psychiatry 2011; 82: 126–35.

Grueter BE, Schulz UG. Age-related cerebral white matter disease (leukoaraiosis): a review. Postgrad Med J 2012; 88: 79–87.

Habes M, Schiller T, Rosenberg C, Burchardt M, Hoffmann W. Automated prostate segmentation in whole-body MRI scans for epidemiological studies. Phys Med Biol 2013; 58: 5899

Hegenscheid K, Kühn JP, Völzke H, Biffar R, Hosten N, Puls R. Whole-body magnetic resonance imaging of healthy volunteers: pilot study results from the population-based SHIP study. RöFo 2009; 181: 748–59.

Ihara M, Polvikoski TM, Hall R, Slade JY, Perry RH, Oakley AE, et al. Quantification of myelin loss in frontal lobe white matter in vascular dementia, Alzheimer's disease, and dementia with Lewy bodies. Acta Neuropathol (Berl) 2010; 119: 579–89.

Jack CRJ, Wiste HJ, Weigand SD, Knopman DS, Mielke MM, Vemuri P, et al. Different definitions of neurodegeneration produce similar amyloid/neurodegeneration biomarker group findings. Brain J Neurol 2015; 138: 3447–59.

Jagust W. Vulnerable neural systems and the borderland of brain aging and neurodegeneration. Neuron 2013; 77: 219–34.

Jeerakathil T, Wolf PA, Beiser A, Massaro J, Seshadri S, D'Agostino RB, et al. Stroke risk profile predicts white matter hyperintensity volume: the Framingham study. Stroke 2004; 35: 1857–61.

Jongen C, van der Grond J, Kappelle LJ, Biessels GJ, Viergever MA, Pluim JPW, et al. Automated measurement of brain and white matter lesion volume in type 2 diabetes mellitus. Diabetologia 2007; 50: 1509–16.

Kievit RA, Davis SW, Mitchell DJ, Taylor JR, Duncan J, Cam-CAN Research Team, et al. Distinct aspects of frontal lobe structure mediate age-related differences in fluid intelligence and multitasking [Internet]. Nat Commun 2014; 5: 5658. Available from: http://dx.doi.org/10.1038/ncomms6658

Klöppel S, Stonnington CM, Chu C, Draganski B, Scahill RI, Rohrer JD, et al. Automatic classification of MR scans in Alzheimer's disease. Brain 2008; 131: 681–9.

Kubicki M, Westin C-F, Maier SE, Frumin M, Nestor PG, Salisbury DF, et al. Uncinate fasciculus findings in schizophrenia: a magnetic resonance diffusion tensor imaging study. Am J Psychiatry 2002; 159: 813–20.

Lao Z, Shen D, Liu D, Jawad AF, Melhem ER, Launer LJ, et al. Computer-assisted segmentation of white matter lesions in 3D MR images using support vector machine. Acad Radiol 2008; 15: 300–13.

Launer LJ, Miller ME, Williamson JD, Lazar RM, Gerstein HC, Murray AM, et al. Effects of intensive glucose lowering on brain structure and function in people with type 2 diabetes (ACCORD MIND): a randomised open-label substudy. Lancet Neurol 2011; 10: 969–77.

Li C, Gore JC, Davatzikos C. Multiplicative intrinsic component optimization (MICO) for MRI bias field estimation and tissue segmentation. Magn Reson Imaging 2014; 32: 913–23.

Longstreth WT, Manolio TA, Arnold A, Burke GL, Bryan N, Jungreis CA, et al. Clinical correlates of white matter findings on cranial magnetic resonance imaging of 3301 elderly people: the cardiovascular health study. Stroke 1996; 27: 1274–82.

Moran C, Phan TG, Chen J, Blizzard L, Beare R, Venn A, et al. Brain atrophy in type 2 diabetes: regional distribution and influence on cognition. Diabetes Care 2013; 36: 4036–42.

Ou Y, Sotiras A, Paragios N, Davatzikos C. DRAMMS: deformable registration via attribute matching and mutual-saliency weighting. Spec Sect 2011; 15: 622–39.

Pennanen C, Testa C, Laakso MP, Hallikainen M, Helkala E-L, Hanninen T, et al. A voxel based morphometry study on mild cognitive impairment. J Neurol Neurosurg Psychiatry 2005; 76: 11–4.

Petrovitch H, Ross GW, Steinhorn SC, Abbott RD, Markesbery W, Davis D, et al. AD lesions and infarcts in demented and non-demented Japanese-American men. Ann Neurol 2005; 57: 98–103.

Prins ND, Scheltens P. White matter hyperintensities, cognitive impairment and dementia: an update. Nat Rev Neurol 2015; 11: 157–65.

Rachael IS, Chris F, Rhian J, Jennifer LW, Martin NR, Nick CF. A longitudinal study of brain volume changes in normal aging using serial registered magnetic resonance imaging. Arch Neurol 2003; 60: 989–94.

Raji CA, Lopez OL, Kuller LH, Carmichael OT, Longstreth WTJ, Gach HM, et al. White matter lesions and brain gray matter volume in cognitively normal elders. Neurobiol Aging 2012; 33

Raz N, Ghisletta P, Rodrigue KM, Kennedy KM, Lindenberger U. Trajectories of brain aging in middle-aged and older adults: regional and individual differences. Neuroimage 2010; 51: 501–11.

Raz N, Lindenberger U, Ghisletta P, Rodrigue KM, Kennedy KM, Acker JD. Neuroanatomical correlates of fluid intelligence in healthy

adults and persons with vascular risk factors. Cereb Cortex 2008; 18: 718–26.
Resnick SM, Pham DL, Kraut MA, Zonderman AB, Davatzikos C. Longitudinal magnetic resonance imaging studies of older adults: a shrinking brain. J Neurosci 2003; 23: 3295–301.
Rosseel Y. lavaan: an R package for structural equation modeling. J Stat Softw 2012; 48: 1–36.
Schmidt R, Ropele S, Enzinger C, Petrovic K, Smith S, Schmidt H, et al. White matter lesion progression, brain atrophy, and cognitive decline: the Austrian stroke prevention study. Ann Neurol 2005; 58: 610–6.
Simpson JE, Fernando MS, Clark L, Ince PG, Matthews F, Forster G, et al. White matter lesions in an unselected cohort of the elderly: astrocytic, microglial and oligodendrocyte precursor cell responses. Neuropathol Appl Neurobiol 2007; 33: 410–9.
Smith EE, O'Donnell M, Dagenais G, Lear SA, Wielgosz A, Sharma M, et al. Early cerebral small vessel disease and brain volume, cognition, and gait. Ann Neurol 2015; 77: 251–61.
Stewart WF, Schwartz BS, Davatzikos C, Shen D, Liu D, Wu X, et al. Past adult lead exposure is linked to neurodegeneration measured by brain MRI. Neurology 2006; 66: 1476–84.
Team RDC. R: a language and environment for statistical computing [Internet]. Vienna, Austria: R Foundation for Statistical Computing; 2008. Available from: http://www.R-project.org
Toledo JB, Arnold SE, Raible K, Brettschneider J, Xie SX, Grossman M, et al. Contribution of cerebrovascular disease in autopsy confirmed neurodegenerative disease cases in the National Alzheimer's Coordinating Centre. Brain 2013; 136: 2697–706.
Toledo JB, Bjerke M, Chen M, Royzycki M, Jack CR, Weiner MW, et al. Memory, executive and multi-domain subtle cognitive impairment: clinical and biomarker findings. Neurology 2015; 85: 144–53.
Toledo J, Weiner M, Wolk D, Da X, Chen K, Arnold S, et al. Neuronal injury biomarkers and prognosis in ADNI subjects with normal cognition. Acta Neuropathol Commun 2014; 2: 26
Tuladhar AM, Reid AT, Shumskaya E, de Laat KF, van Norden AGW, van Dijk EJ, et al. Relationship between white matter hyperintensities, cortical thickness, and cognition. Stroke J Cereb Circ 2015; 46: 425–32.
Tullberg M, Fletcher E, DeCarli C, Mungas D, Reed BR, Harvey DJ, et al. White matter lesions impair frontal lobe function regardless of their location. Neurology 2004; 63: 246–53.
Tustison NJ, Avants BB, Cook P, Zheng Y, Egan A, Yushkevich P, et al. N4ITK: improved N3 bias correction. IEEE Trans Med Imaging 2010; 29: 1310–20.
Van der Flier WM, van Straaten ECW, Barkhof F, Ferro JM, Pantoni L, Basile AM, et al. Medial temporal lobe atrophy and white matter hyperintensities are associated with mild cognitive deficits in non-disabled elderly people: the LADIS study. J Neurol Neurosurg Psychiatry 2005; 76: 1497–500.
Vapnik V. The nature of statistical learning theory (Information Science and Statistics), 2nd ed. Berlin, Germany: Springer Science & Business Media; 1999.
Vemuri P, Gunter JL, Senjem ML, Whitwell JL, Kantarci K, Knopman DS, et al. Alzheimer's disease diagnosis in individual subjects using structural MR images: validation studies. Neuroimage 2008; 39: 1186–97.
Vemuri P, Simon G, Kantarci K, Whitwell JL, Senjem ML, Przybelski SA, et al. Antemortem differential diagnosis of dementia pathology using structural MRI: differential-STAND. Neuroimage 2011; 55: 522–31.
Verhaaren BFJ, Debette S, Bis JC, Smith JA, Ikram MK, Adams HH, et al. Multi-ethnic genome-wide association study of cerebral white matter hyperintensities on MRI [Internet]. Circ Cardiovasc Genet 2015; 8: 398–406. Available from: http://circgenetics.ahajournals.org/content/early/2015/02/07/CIRCGENETICS.114.000858.abstract
Vermeer SE, Prins ND, den Heijer T, Hofman A, Koudstaal PJ, Breteler MMB. Silent brain infarcts and the risk of dementia and cognitive decline. N Engl J Med 2003; 348: 1215–22.
Völzke H, Alte D, Schmidt CO, Radke D, Lorbeer R, Friedrich N, et al. Cohort profile: the study of health in pomerania [Internet]. Int J Epidemiol 2011; 40: 294–307. Available from: http://ije.oxfordjournals.org/content/early/2010/02/18/ije.dyp394.short
Wang R, Fratiglioni L, Laveskog A, Kalpouzos G, Ehrenkrona C-H, Zhang Y, et al. Do cardiovascular risk factors explain the link between white matter hyperintensities and brain volumes in old age? A population-based study. Eur J Neurol 2014; 21: 1076–82.
Wang W-Y, Yu J-T, Liu Y, Yin R-H, Wang H-F, Wang J, et al. Voxel-based meta-analysis of grey matter changes in Alzheimer's disease. Transl Neurodegener 2015; 4: 6.
Wardlaw JM, Allerhand M, Doubal FN, Valdes Hernandez M, Morris Z, Gow AJ, et al. Vascular risk factors, large-artery atheroma, and brain white matter hyperintensities. Neurology 2014; 82: 1331–8.
Wardlaw JM, Pantoni L. Sporadic small vessel disease: pathogenic aspects [Internet]. In: Cerebral Small Vessel Disease. Cambridge: Cambridge University Press; 2014. p. 52. Available from: http://dx.doi.org/10.1017/CBO9781139382694.007
Wardlaw JM, Valdés Hernández MC, Muñoz_Maniega S. What are White matter hyperintensities made of? Relevance to vascular cognitive impairment [Internet]. J Am Heart Assoc 2015; 4: 001140. Available from: http://jaha.ahajournals.org/content/4/6/001140.short
Wardlaw J, Smith C, Dichgans M. Mechanisms underlying sporadic cerebral small vessel disease: insights from neuroimaging. Lancet Neurol 2013; 12: 10–1016/S1474–4422(13)70060–7.
Wen W, Sachdev PS, Chen X, Anstey K. Gray matter reduction is correlated with white matter hyperintensity volume: a voxel-based morphometric study in a large epidemiological sample. Neuroimage 2006; 29: 1031–9.
Wirth M, Villeneuve S, Haase CM, Madison CM, Oh H, Landau SM, et al. Associations between Alzheimer disease biomarkers, neurodegeneration, and cognition in cognitively normal older people. JAMA Neurol 2013; 70: 1512–9.
Woods SP, Delis DC, Scott JC, Kramer JH, Holdnack JA. The California Verbal Learning Test – second edition: test-retest reliability, practice effects, and reliable change indices for the standard and alternate forms. Arch Clin Neuropsychol 2006; 21: 413–20.
Zhang T, Davatzikos C. ODVBA: optimally-discriminative voxel-based analysis. IEEE Trans Med Imaging 2011; 30: 1441–54.
Zhang T, Davatzikos C. Optimally-discriminative voxel-based morphometry significantly increases the ability to detect group differences in schizophrenia, mild cognitive impairment, and Alzheimer's disease. Neuroimage 2013; 79: 94–110.